



**AFRL-RX-WP-JA-2014-0224**

**CHARACTERIZATION OF MICROSTRUCTURE WITH  
LOW FREQUENCY ELECTROMAGNETIC  
TECHNIQUES (POSTPRINT)**

**Matthew R. Cherry and Shamachary Sathish  
University of Dayton Research Institute**

**Aaron J. Cherry  
Southwestern Ohio Council for Higher Education**

**Adam L. Pilchak and Mark P. Blodgett  
AFRL/RXCA**

**AUGUST 2013  
Interim Report**

**Distribution A. Approved for public release; distribution unlimited.**

*See additional restrictions described on inside pages*

**STINFO COPY**

**© 2014 AIP Publishing LLC**

**AIR FORCE RESEARCH LABORATORY  
MATERIALS AND MANUFACTURING DIRECTORATE  
WRIGHT-PATTERSON AIR FORCE BASE, OH 45433-7750  
AIR FORCE MATERIEL COMMAND  
UNITED STATES AIR FORCE**



# REPORT DOCUMENTATION PAGE

Form Approved  
OMB No. 074-0188

Public reporting burden for this collection of information is estimated to average 1 hour per response, including the time for reviewing instructions, searching existing data sources, gathering and maintaining the data needed, and completing and reviewing this collection of information. Send comments regarding this burden estimate or any other aspect of this collection of information, including suggestions for reducing this burden to Defense, Washington Headquarters Services, Directorate for Information Operations and Reports, 1215 Jefferson Davis Highway, Suite 1204, Arlington, VA 22202-4302. Respondents should be aware that notwithstanding any other provision of law, no person shall be subject to any penalty for failing to comply with a collection of information if it does not display a currently valid OMB control number. PLEASE DO NOT RETURN YOUR FORM TO THE ABOVE ADDRESS.

<b>1. REPORT DATE (DD-MM-YYYY)</b> August 2013		<b>2. REPORT TYPE</b> Interim		<b>3. DATES COVERED (From - To)</b> 25 June 2009 - 21 July 2013	
<b>4. TITLE AND SUBTITLE</b> CHARACTERIZATION OF MICROSTRUCTURE WITH LOW FREQUENCY ELECTROMAGNETIC TECHNIQUES (POSTPRINT)				<b>5a. CONTRACT NUMBER</b> FA8650-09-D-5224-0001	
				<b>5b. GRANT NUMBER</b>	
				<b>5c. PROGRAM ELEMENT NUMBER</b> 62102F	
<b>6. AUTHOR(S)</b> (see back)				<b>5d. PROJECT NUMBER</b> 4347	
				<b>5e. TASK NUMBER</b>	
				<b>5f. WORK UNIT NUMBER</b> X0SU	
<b>7. PERFORMING ORGANIZATION NAME(S) AND ADDRESS(ES)</b> (see back)				<b>8. PERFORMING ORGANIZATION REPORT NUMBER</b>	
<b>9. SPONSORING / MONITORING AGENCY NAME(S) AND ADDRESS(ES)</b> Air Force Research Laboratory Materials and Manufacturing Directorate Wright Patterson Air Force Base, OH 45433-7750 Air Force Materiel Command United States Air Force				<b>10. SPONSOR/MONITOR'S ACRONYM(S)</b>  AFRL/RXCA	
				<b>11. SPONSOR/MONITOR'S REPORT NUMBER(S)</b> AFRL-RX-WP-JA-2014-0224	
<b>12. DISTRIBUTION / AVAILABILITY STATEMENT</b> Distribution A. Approved for public release; distribution unlimited. This report contains color.					
<b>13. SUPPLEMENTARY NOTES</b> Journal article published in AIP Conf. Proc. 1581, 1456-1462 (2014) © 2014 AIP Publishing LLC 978-7354-1211-8. The U.S. Government is joint author of the work and has the right to use, modify, reproduce, release, perform, display or disclose the work. The final publication is available at doi: 10.1063/1.4864993. If authorized, also see also AFRL-RX-WP-TR-2014-0218. Preprint is AFRL-RX-WP-TM-2014-0065.					
<b>14. ABSTRACT</b> A new computational method for characterizing the relationship between surface crystallography and electrical conductivity in anisotropic materials with low frequency electromagnetic techniques is presented. The method is discussed from the standpoint of characterizing the orientation of a single grain, as well as characterizing statistical information about grain ensembles in the microstructure. Large-area electron backscatter diffraction (EBSD) data was obtained and used in conjunction with a synthetic aperture approach to simulate the eddy current response of beta annealed Ti-6Al-4V. Experimental eddy current results are compared to the computed eddy current approximations based on electron backscatter diffraction (EBSD) data, demonstrating good agreement. The detectability of notches in the presence of noise from microstructure is analyzed with the described simulation method and advantages and limitations of this method are discussed relative to other NDE techniques for such analysis.					
<b>15. SUBJECT TERMS</b> eddy current, microstructure, hexagonal, anisotropic					
<b>16. SECURITY CLASSIFICATION OF:</b>			<b>17. LIMITATION OF ABSTRACT</b>  SAR	<b>18. NUMBER OF PAGES</b>  11	<b>19a. NAME OF RESPONSIBLE PERSON (Monitor)</b> John T. Welter
<b>a. REPORT</b> Unclassified	<b>b. ABSTRACT</b> Unclassified	<b>c. THIS PAGE</b> Unclassified			<b>19b. TELEPHONE NUMBER (include area code)</b> (937) 255-9798

## REPORT DOCUMENTATION PAGE Cont'd

### 6. AUTHOR(S)

Matthew R. Cherry and Shamachary Sathish  
University of Dayton Research Institute

Aaron J. Cherry  
Southwestern Ohio Council for Higher Education

Adam L. Pilchak and Mark P. Blodgett  
AFRL/RXCA

### 7. PERFORMING ORGANIZATION NAME(S) AND ADDRESS(ES)

University of Dayton Research Institute  
Structural Integrity Division  
300 College Park Drive  
Dayton OH 45469

Southwestern Ohio Council for Higher Education  
Dayton, OH 45420

AFRL/RXCA  
Air Force Research Laboratory  
Materials and Manufacturing Directorate  
Wright-Patterson Air Force Base, OH 45433-7750

# Characterization of Microstructure with Low Frequency Electromagnetic Techniques

Matthew R. Cherry<sup>b</sup>, Shamachary Sathish<sup>b</sup>, Adam L. Pilchak<sup>a</sup>, Aaron J. Cherry<sup>c</sup>,  
and Mark P. Blodgett<sup>a</sup>

<sup>a</sup>*Air Force Research Laboratory, Materials and Manufacturing Directorate (AFRL/RXCM)  
2230 10<sup>th</sup> St., WPAFB, OH 45433, USA*

<sup>b</sup>*University of Dayton Research Institute, Structural Integrity Division  
300 College Park, Dayton, OH 45469-0020, USA*

<sup>c</sup>*Southwest Ohio Council for Higher Education  
3155 Research Blvd., Suite 204, Dayton, OH 45420-4015, USA*

**Abstract.** A new computational method for characterizing the relationship between surface crystallography and electrical conductivity in anisotropic materials with low frequency electromagnetic techniques is presented. The method is discussed from the standpoint of characterizing the orientation of a single grain, as well as characterizing statistical information about grain ensembles in the microstructure. Large-area electron backscatter diffraction (EBSD) data was obtained and used in conjunction with a synthetic aperture approach to simulate the eddy current response of beta annealed Ti-6Al-4V. Experimental eddy current results are compared to the computed eddy current approximations based on electron backscatter diffraction (EBSD) data, demonstrating good agreement. The detectability of notches in the presence of noise from microstructure is analyzed with the described simulation method and advantages and limitations of this method are discussed relative to other NDE techniques for such analysis.

**Keywords:** Eddy Current, Microstructure, Hexagonal, Anisotropic  
**PACS:** 81.70.-q, 81.05.Xj

## INTRODUCTION

One of the main confounding factors in using the methods of eddy current testing (ECT) to detect small ( $< 0.1$  mm) cracks in engineering anisotropic alloys is the microstructure of the material. When the change of impedance due to the presence of the crack is on the same order as the change due to perturbations in crystallographic orientation, the crack signal gets lost in what is often perceived as the surrounding “grain noise” [1]. This situation is illustrated in Fig 1. The same sized electrical discharge machined (EDM) notch was scanned in two different materials. The main difference between the two images is that the material in the image on the left is isotropic vs. the anisotropic material on the right. Several methods could be used to enhance the signal from the notch in Fig. 1(b). Any of several image processing routines could be used to identify and subtract the features caused by the microstructure from that due to the presence of damage. This would offer some sensitivity to the notch or it could provide a method to reduce the noise. This would be a similar approach to using spatial Fourier transforms to extract features from images. These methods do offer some enhanced sensitivity to the notch signal, but in the process they make parameter estimation much more involved. For NDE purposes, the ideal situation is one in which this data can be used in its raw form to estimate characteristics of the damage. For this type of analysis, a thorough understanding of the physics involved is



FIGURE 1. Eddy current scans taken over the same sized crack in (a) AL 2024 and in (b) Ti-6Al-4V ( $\beta$  annealed) [1].

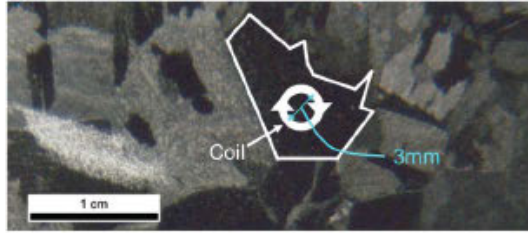


FIGURE 2. Image of the sample analyzed in this work. The grains are clearly large enough that the coil can resolve them.

extremely helpful. To this end, this work is mainly concerned with proof of the theory that this noise is related to microstructure and in providing a potential forward model approximation for this type of problem.

## EXPERIMENTS

Experiments were performed initially to determine the source of the material noise and then to provide sample information to the forward models for verification. An appropriate sample was chosen for the purposes of the work, and then several different experimental techniques were used to collect information about the microstructure. The different experimental data sets were compared for verification.

### Sample

In order to illustrate and exacerbate the role of grain orientation on conductivity, thereby demonstrating the source of microstructure-induced noise, a coarse-grained beta-annealed Ti-6Al-4V sample was selected for this work. The grains were sufficiently large that the diameter of a standard, commercially available ECT probe was less than the typical grain diameter and therefore the signal at a given could be due to a single grain. It is noteworthy that the large grain dimensions, up to  $\sim 1$  cm, in this sample imply a large radius of curvature of the colony boundaries, much larger, in fact, than the depth contributing to the eddy current signal and thus complications due to subsurface variations in orientation that may be present in fine grained materials were not a source of variability here. The optical images of the sample shown in Fig. 2 illustrate this point more clearly. Ti-6Al-4V consists primarily of the hexagonal close packed  $\alpha$ -phase ( $\sim 93\%$  volume fraction) with the remainder balanced by the body center cubic  $\beta$ -phase. The  $\alpha$ -phase exhibits isotropy in the basal plane, but most physical properties are moderately anisotropic and depend on angle relative to the  $[0001]$  (c-axis) direction. The variation in conductivity from the basal plane to the c-axis is nominally about 6% difference, and the conductivity in the basal plane is assumed to be on the order of  $2.4 \times 10^6$  S/m [2].

### Electron Backscatter Diffraction

Since most properties vary as a function of orientation, and the cost of these measurements is becoming more affordable, large-area microstructure characterization involving measurement of local orientation via EBSD is becoming increasingly commonplace (e.g. [3]). Crystallographic orientation in an orthonormal basis can be fully

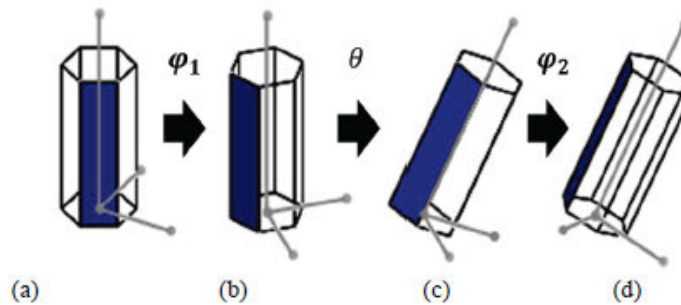


FIGURE 3. (a) The hexagonal crystal in an orientation in line with the sample axes, (b) rotated an angle  $\varphi_1$  about the initial z-axis, (c) rotated an angle  $\theta$  about the new x-axis, and (d) rotated an angle  $\varphi_2$  about the newest z-axis.

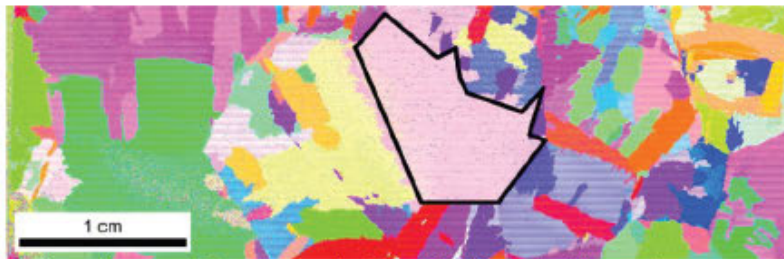


FIGURE 4. Crystal orientation map of the coarse-grained Ti-6Al-4V sample. Here, color corresponds to crystallographic orientation. The large grain in the center is outlined for reference.

described by a set of Euler angles  $(\varphi_1, \theta, \varphi_2)$  in Bunge's active form, as shown in Fig. 3. The Euler angles essentially define the rotations necessary to bring the sample axes into coincidence with an arbitrarily oriented crystal [4]. In this work, a direct comparison between eddy current images and the actual sample cannot be made without this orientation information. Orientation data were collected with electron backscatter diffraction using a Phillips XL30 scanning electron microscope (SEM) operated at an accelerating voltage of 20 kV at a probe current of 50 nA. The resulting data is shown in Fig 4.

### Eddy Current Experiments

A commercially available, 2MHz center frequency probe was used to collect ECT data from the large grained sample shown above. The probe was connected to a Nortec 2000D eddy current scope and raster scanned over the entire specimen. This combination of instrument and probe has been shown to produce detectable signals from conductivity changes of below 6%, which is the maximum change that would be expected from the sample (i.e. the percent difference between the c-axis and the basal plane conductivities). To achieve such sensitive measurements, one crucial step is to determine the probe's sensitivity to conductivity vs. liftoff. A calibration curve for this probe generated with physical models [5] can be seen in Fig. 5. The conductivity range that the sample is in is close to 1.75 %IACS, which, upon inspection of the curve in that range, means that liftoff is not orthogonal to conductivity changes. However, with conductivity changes on the order of 6% [2], the magnitude change is close enough to linear to use it as the impedance measurement. Liftoff was controlled by using the probe in contact with the specimen. An image of the magnitude of impedance above the sample is shown in Fig. 6. This image shows some of the grains that can be seen in the OIM image indicating that the ECT method is capable of distinguishing the grains, and that the change in the impedance of the coil is due mainly to the conductivity change from one region to another.

### APPROXIMATION METHOD

Knowing that this variation in impedance measurements over Ti and its alloys is a conductivity variation due to microstructure, a quick and accurate approximation method for forward models of this phenomenon can be obtained. This is useful if statistical quantification of the microstructure is to be accomplished with ECT methods. The key to the approximation lies in several assumptions that will be enumerated here to clarify the method as well as provide potential avenues to refine the approximation.

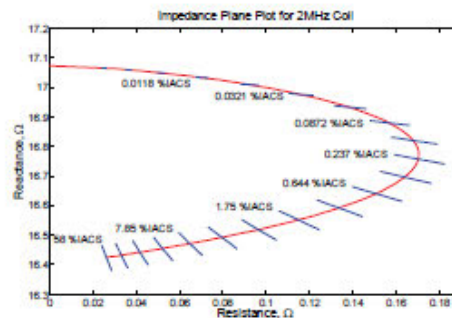


FIGURE 5. Calibration curve for the eddy current probe. The curve represents change in conductivity, and the hash marks represents a change in liftoff at a fixed conductivity.

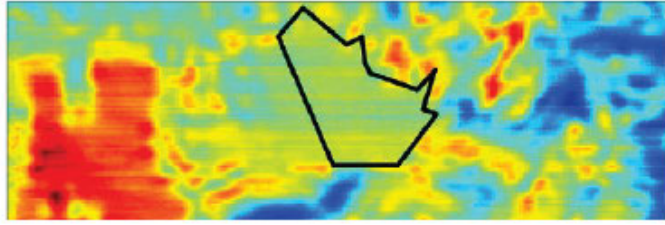


FIGURE 6. ECT scan of the sample.

### Assumption 1: Uniform Electric Field

This assumption states that underneath the coil, the electric field is uniform inside the conductor. This is an assumption since, as can be seen in any mathematical analysis of eddy current problems [6, 7], the electric field in the conductor is dependent on the conductivity of the sample. However, this assumption hinges on the fact that the conductivity changes are so small that the variation of electric field from one grain to the other is small. The definition of “small enough” here is not analyzed, and in fact this assumption might be fairly stringent. However, since the goal is to produce an approximation of an eddy current scan, this assumption will be enforced.

### Assumption 2: No Changes in Depth

The second assumption is that the grains that we see in the EBSD map are “pillars”, or that they are constant in the depth of the sample. This is clearly a strict and rather limiting assumption. The skin depth of the eddy currents in this material at 2MHz is around 230 $\mu$ m. Common commercially used Ti alloys have microstructures with grain sizes in the range of 10-20 $\mu$ m meaning that the present analysis would be confounded by non surface-connected grains which would contribute to the eddy current response. In this case, however, the large grain size and commensurate large grain boundary curvature implies that the region of constant orientation far exceeds the depth of the eddy currents. Optical inspection of both sides of the sample indicated that many of the grains actually spanned the entire thickness (~5 mm) validating that assumption that the EBSD measurements are representative of the orientations at least.

### Details of the Method

With the assumptions clear, the approximation routine can now be elaborated upon. The first thing that must be understood is that the conductivity in the material is different for electric fields of different direction. The constitutive relation for induced current density in the presence of an electric field is [8]:

$$J = \sigma E \quad (1)$$

$J$  is the current density,  $\sigma$  is the conductivity tensor, and  $E$  is the electric field. If we assume an electric field in the direction of a unit direction vector,  $r$ , and assign it some arbitrary magnitude, say  $E_{mag}$ , then with some steps of linear algebra, the magnitude of the current density induced can be expressed as:

$$J_{mag} = E_{mag}(r^T \sigma^2 r)^{1/2} \quad (2)$$

This expresses the magnitude of the current density as a function of an electric field in an arbitrary direction and the conductivity tensor of the sample. The current density here is not necessarily in the direction of the electric field, but its magnitude is correct. We can define an effective conductivity as  $\sigma_{eff} = (r^T \sigma^2 r)^{1/2}$ . When the electric field is in the direction of one of the principal axes of the conductivity tensor, the conductivity comes out as the single crystal conductivity in that direction, as expected. Now, for an arbitrary set of rotations given Euler angles, a rotation matrix for the conductivity tensor can be defined as [4]:

$$R = \begin{bmatrix} c_1 c_3 - c_2 s_1 s_3 & -c_1 s_3 - c_2 c_3 s_1 & s_1 s_2 \\ c_3 s_1 + c_1 c_2 s_3 & c_1 c_2 c_3 - s_1 s_3 & -c_1 s_2 \\ s_2 s_3 & c_3 s_2 & c_2 \end{bmatrix}^T \quad (3)$$

C represents cosine and s represents sine, and the subscripts 1, 2, and 3 represent the operations on Euler angles  $\varphi_1$ ,  $\theta$ , and  $\varphi_2$  respectively. Given a new direction,  $Rr$ , for the electric field, the electric field can be expressed as:

$$E = E_{mag} Rr \quad (4)$$

Again, we write the constitutive relation for the newly aligned region as:

$$J = \sigma E = E_{mag} \sigma Rr \quad (5)$$

We can carry out the same operations for an electric field in an arbitrary direction and arrive at a final expression for the magnitude of the current density as:

$$J_{mag} = E_{mag} (r^T R^T \sigma^2 Rr)^{1/2} \quad (6)$$

where we've used the fact that  $R^{-1} = R^T$ . The effective conductivity in this expression:

$$\sigma_{eff} = (r^T R^T \sigma^2 Rr)^{1/2} \quad (7)$$

represents the conductivity in the direction of the electric field.

With this definition of effective conductivity, an expression for the conductivity of a point below the coil can be derived. The first assumption implies that the field below the coil and in the sample flows tangential to the coil. This is a similar assumption to that made when solving an axisymmetric problem with scalar conductivities as in [5]. With that in mind, the direction of the electric field at a point,  $p_i$ , below the coil can be calculated by drawing a line to the point and then drawing the normal line to that point in the direction opposite the flow of currents in the coil (due to Lenz's law, though the direction doesn't matter in this application). The schematic of this is shown in Fig. 7. Setting the coil center as the origin (0,0) and calling the vector to the point  $d_i$ , the equation for the tangential direction,  $r_i$ , can be written as:

$$r_i = \frac{[0 \ 0 \ 1] \times d_i}{|d_i|} = \frac{[-d_y \ d_x \ 0]}{|d_i|} \quad (8)$$

This value of  $r_i$ , along with the Euler angles at the point are then use in equation 7 to calculate the effective conductivity at that point. Since the OIM data is a regular grid of points, averaging every point below the coil gives what is similar to an area-weighted average of orientation-dependent conductivities. This average, when plotted for every coil position, gives an estimate of what an ECT scan would look like above an anisotropic material. This essentially amounts to a synthetic aperture approach for eddy current scans above a conductive medium with subtle variations in conductivity.

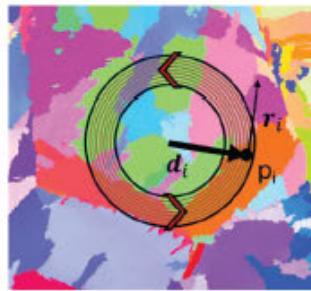


FIGURE 7. The direction of the electric field used in effective conductivity calculations at a point,  $p_i$ , below the coil.

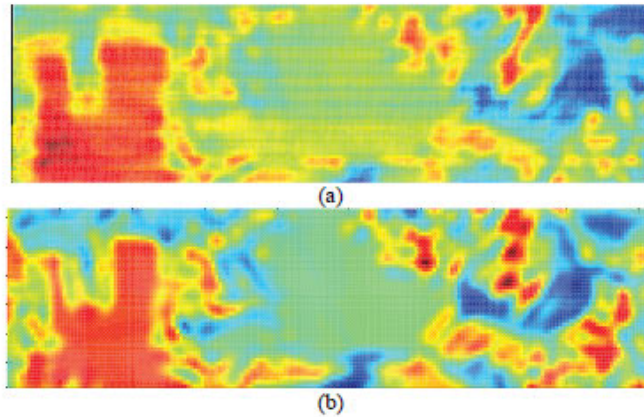


FIGURE 8. Images of (a) an actual ECT scan of the sample and (b) a simulated ECT scan.

### COMPARISONS AND VERIFICATION

To test the synthetic aperture routine, the Euler angles that were collected from the sample were fed into the numerical method and a simulated eddy current scan was performed. The images are shown back-to-back in Fig 8. There are some features that are clearly visible in both images, but other regions are very difficult to compare. The cause of this is partly the fact that the first assumption implies that the results of the simulation are not physically accurate, and that the 3D grain morphology is missing from the simulation. Again, since the grains are mostly large enough, the second assumption is not as crucial, but it could be relevant if the angle of the grain boundary is drastic in depth. Further validation to estimate the effect of the assumptions would require 3D sectioning experiments and the use of a full numerical solution such as finite element method (FEM), boundary element method (BEM), or volume integral method (VIM). As of writing this paper, these experiments have not been performed.

On the other hand, this type of verification has been demonstrated to a lesser extent with FEM methods. A problem with the geometry and conductivities shown in Fig. 9 was analyzed with COMSOL Multiphysics. The details of this model can be found in [9]. The two different conductivity regions were simulated using a different rotation matrix for each. The FEM simulation gives changes in impedance of the coil, whereas the synthetic aperture routine give changes in conductivity. However, it was already shown that this relationship can be considered linear with such small changes in conductivity, so the results from each were normalized and plotted in Fig. 10. The synthetic aperture routine shows very good agreement with the FEM results.

### CONCLUSIONS, DISCUSSION, AND FUTURE WORK

From the data provided in this paper, it is reasonable to conclude that noise in the scans shown is likely due to microstructure changes in an anisotropic material. This conclusion has been reach by other authors, but no direct comparison between OIM and eddy current scans has been made. The OIM maps of these scans offer insight into the actual composition of the sample, as well as give quantitative information that can be used in the context of forward models. The approximation method shown here has potential to expedite these forward model solutions by providing the ECT information over the microstructure. This bodes well for future inversion schemes that may take advantage of the physical intuition of anisotropic material noise. Incorporation of this into parameter estimation routines remains as future work. First and foremost, a very thorough investigation of the validity of the assumptions made must be undertaken and the approximation method must be validated with real experimental data.

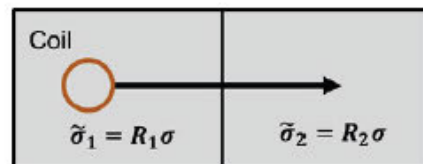


FIGURE 9. Image of the geometry analyzed with the FEM model as well as the approximation method.

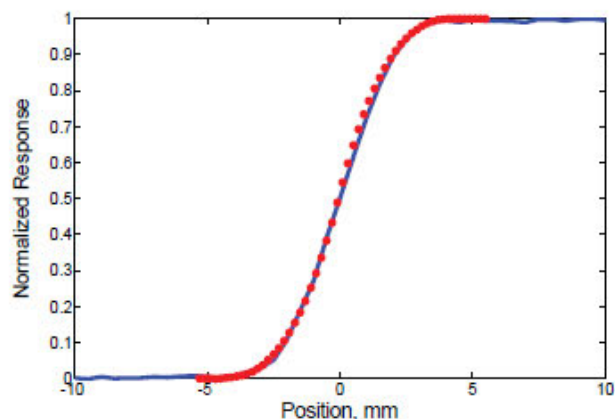


FIGURE 10. Results from the FEM model is represented by dots, and results from the synthetic aperture routine are shown as a line.

### ACKNOWLEDGMENTS

The authors would like to acknowledge support from funding under USAF contracts FA8650-09-D-5224 and FA8650-09-2-5800.

### REFERENCES

1. M. P. Blodgett, W. Hassan, P. B. Nagy, "Theoretical and experimental investigations of the lateral resolution of eddy current imaging", *Materials Eval.*, pp. 647-654 (2000).
2. G. T. Meaden, "Electrical Resistance of Metals", Plenum, New York (1965).
3. G. A. Sargent, K. T. Kinsel, A. L. Pilchak, A. A. Salem, S. L. Semiatin, "Variant Selection During Cooling after Beta Annealing of Ti-6Al-4V Ingot Material", *Metallurgical and Materials Transactions A*, Vol. 43 No. 10, pp. 3570-3585.
4. Kocks, U. F., Tomé, C. N., and Wenk, H. R. (Eds.), "Texture and anisotropy: preferred orientations in polycrystals and their effect on materials properties", Cambridge university press (2000).
5. Theodoulidis, T., & Kriezis, E., "Series expansions in eddy current nondestructive evaluation models", *Journal of materials processing technology*, 161(1), pp. 343-347 (2005).
6. Libby, H. L., "Introduction to Electromagnetic Nondestructive Test Methods", Wiley-Interscience, New York (1971).
7. Coffey, M. W., "Theory for coil impedance of a conducting half space: Analytic results for eddy current analysis", *J. Appl. Phys.* 89, p. 2473 (2001).
8. Cheng, D. K., "Field and Wave Electromagnetics", Addison-Wiley Publishing Company, Inc., (1989).
9. Cherry, M. R., Mooers, R., Knopp, J., Aldrin, J. C., Sabbagh, H. A., Boehnlein, T., "Low frequency eddy current finite element model validation and benchmark studies", *Review of Progress in Nondestructive Testing*, AIP Conf. Proc. 1335, pp. 357-364.